



## A REGIONAL GEOMAGNETIC MODEL USING FOURIER ANALYSIS

R. Jayapal<sup>1</sup>, Shenu Gopal<sup>2</sup>, C. P. Anilkumar<sup>3</sup> & Chandu Venugopal<sup>2</sup>

<sup>1</sup>Department of Physics, D B College, Thalayolapparambu, Kerala - 686 605, India.

<sup>2</sup>School of Pure & Applied Physics, Mahatma Gandhi University, Priyadarshini Hills,  
Kottayam -686560, Kerala, India.

<sup>3</sup>Equatorial Geophysical Research Laboratory, Indian Institute of Geomagnetism, Krishnapuram,  
Tirunelveli – 627 011, Tamil Nadu, India.

### **ABSTRACT**

*We have Fourier analysed the horizontal component (H) of the Earth's magnetic field at Thiruvananthapuram (lat. 8° 29' N, long. 76° 59' E) during the years 1987 to 1998. The infinite number of terms in the Fourier expansion was truncated after the fifth term for both magnetically "quiet" and "disturbed" days.*

*We find that terms up to order 5 are sufficient to model the observed magnetic field at Thiruvananthapuram during both magnetically quiet and disturbed days, as there is an excellent agreement between the observed and the Fourier analysed and reconstructed fields. The seasonal and solar cycle dependence of the Fourier amplitudes have also been studied; we find the Fourier amplitudes are well correlated with the sunspot numbers.*

**KEYWORDS** – Geomagnetic field, Model, Fourier Analysis, Equatorial Station

### **INTRODUCTION**

Models of the geomagnetic field use mathematical expressions to represent space and time variations of the Earth's magnetic field. Starting from the classical technique of Spherical Harmonic Analysis (SHA), first introduced by Gauss, considerable progress has been made in modelling the quiet-time, near-Earth magnetic field. For example, data from four satellites

(POGO, Magsat, Orsted and Champ) were used to construct a sophisticated model that could separate out various field sources [1].

Past attempts have used Harmonic (Fourier) Analysis (HA) to model the solar quiet ( $S_q$ ) variation [2, 3]. Other methods such as Rectangular Harmonic Analysis [4] , Spherical Cap Harmonic Analysis (SCHA) [5] have also been used. Spherical harmonic analyses has been further augmented by a physical method of regularization [6] and the revised Spherical Cap Harmonic Analysis (R-SCHA) [7]. Still other methods such as wavelet analysis [8] and Artificial Neural Networks (ANN) techniques [9] have also been used to model the geomagnetic daily variations.

In this paper we use the conventional HA method to model the horizontal component of the geomagnetic field observed at Thiruvananthapuram (lat  $8^\circ 29'$  N, long  $76^\circ 59'$  E) during the years 1987 – 1998. We find that the first 5 harmonics in the Fourier expansion models very well the horizontal component of the Earth’s magnetic field during both geomagnetically quiet as well as disturbed days. The seasonal and solar cycle dependence of the Fourier amplitudes have also been studied.

## DATA ANALYSIS

As mentioned above we are interested in the HA of the horizontal component (H-component) of the Earth’s magnetic field observed at Thiruvananthapuram (lat  $8^\circ 29'$  N, long  $76^\circ 59'$  E) during the period 1987 – ’98. The data thus consists of 24 values of the H-component for a day.

## HARMONIC ANALYSIS

A time dependent harmonic function  $F(t)$  with 24 equidistant points in the interval from  $t = 0$  to  $t = 24 (2\pi)$  can be expressed as

$$F(t_n) = \frac{A_0}{2} + \sum_{p=1}^{N/2} A_p \cos(\omega_p t) + B_p \sin(\omega_p t) \quad (1)$$

where the time, time-step and trigonometric arguments are given by

$$t_n = n \Delta t \ ; \ \Delta t = T / N \ ; \ \omega_p t = 2 \pi p n / N \quad (2)$$

The expressions for  $A_0$ ,  $A_p$ , and  $B_p$  are given by

$$A_0 = \frac{2}{N} \sum_{n=1}^N F(t_n)$$

$$A_p = \frac{2}{N} \sum_{n=1}^N F(t_n) \cos\left(\frac{2\pi p n}{N}\right) ; p \neq \frac{N}{2} ;$$

$$A_p = \frac{1}{N} \sum_{n=1}^N F(t_n) \cos\left(\frac{2\pi n (N/2)}{N}\right) ; p = \frac{N}{2} ;$$

and

$$B_p = \frac{2}{N} \sum_{n=1}^N F(t_n) \sin\left(\frac{2\pi p n}{N}\right) ; p = 1, 2, \dots, \frac{N}{2} - 1 \quad (3)$$

The amplitude  $C_p$  and phase  $\phi_p$  of the  $p^{\text{th}}$  harmonic are then given by

$$C_p = \left[ A_p^2 + B_p^2 \right]^{1/2}$$

$$\text{and } \phi_p = \tan^{-1}( B_p / A_p ) \quad (4)$$

The daily variations of the horizontal component of Earth's magnetic field can then be expressed

as

$$F(t_n) = \frac{A_0}{2} + A_1 \cos\left(\frac{2\pi n}{N}\right) + B_1 \sin\left(\frac{2\pi n}{N}\right) + A_2 \cos\left(\frac{4\pi n}{N}\right) + B_2 \sin\left(\frac{4\pi n}{N}\right) + \dots \quad (5)$$

## DATA CORRECTION

The daily variation in the H-field is not strictly periodic as required by Fourier analysis; that is, the H-value at  $t=1$  hour will not, in general, be the same for  $t=25$  hours. This difference, which is due to many factors, is corrected for in practice by applying a correction for non-cyclic behavior, the details of which are given below [10].

The base line for the H-field is defined as the average of the four values flanking local midnight (23, 24, 1 and 2 hours). The daily base line values used in this paper are:

$$H_0 = ( H_{23} + H_{24} + H_1 + H_2 ) / 4 \quad (6)$$

where  $H_0$  is rounded off to the nearest whole number while  $H_1, H_2, H_{23}$  and  $H_{24}$  are the hourly H-values at 1, 2, 23 and 24 hours local time respectively.

The hourly departures of the H-field from the midnight baseline value defined by (6) were obtained by subtracting (6) for a particular day from the hourly values for that particular day. Thus at “t” hours LT

$$\Delta H_t = H_t - H_0 \quad (7) \quad \text{where } t = 1 \text{ to } 24 \text{ hours.}$$

The hourly departure was further corrected for the noncyclic variation mentioned above. This was done by making a linear adjustment in the daily hourly values of  $\Delta H$ . Thus if the hourly departures of  $\Delta H$  at 01 LT, 02 LT, ....., 24 LT are denoted as  $V_1, V_2, \dots, V_{24}$ , the linearly adjusted values at these hours are [10]

$$V_{1+0\Delta_c}, V_{2+1\Delta_c}, V_{3+2\Delta_c}, \dots, V_{24+23\Delta_c} \quad \text{where } \Delta_c = \frac{V_1 - V_{24}}{23}$$

$$\text{Or, in other words, } \Delta H_t(V) = \Delta H_t - (t - 1)\Delta_c \quad (8)$$

Here  $t$  is the time, ranging from 01 to 24.

## RESULTS

The final corrected values of the H-field, as given by (8), were Fourier analysed using (4) and reconstructed using (5), the analysis being restricted to “quiet” and “disturbed” days. The mean monthly hourly variations were arrived at by finding the mean of the hourly  $\Delta H_t(V)$  values for each set of five “quiet” days of each month and similarly for the “disturbed” days.

Figure 1 is a plot of the observed data values (indicated by “continuous lines”) and the Fourier analyzed and reconstructed data values (indicated by “dashed lines”) versus UT for quiet

days of January, 1987. The reconstructed data contains the first 5 harmonics in the Fourier series of (5). As can be seen from the figure, the  $\Delta H_i(V)$  or H-field values increases with increasing time, reaches a maximum between 07 - 08 UT declines sharply and reaches the baseline value by about 1500 hrs UT

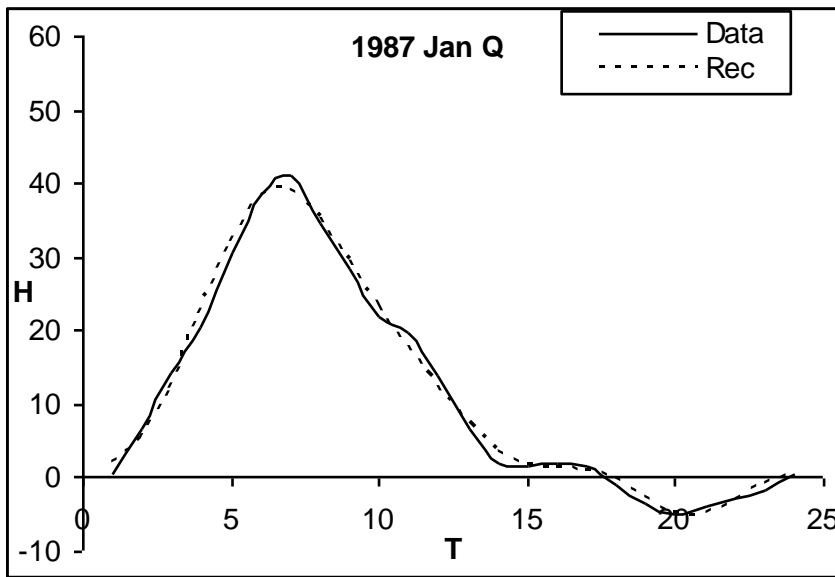


Figure 1: Plot of the measured values of the horizontal component of the earth's magnetic field (indicated by the continuous curve) and the Fourier analysed and reconstructed values (indicated by the dashed curve) for the five quiet days of January, 1987.

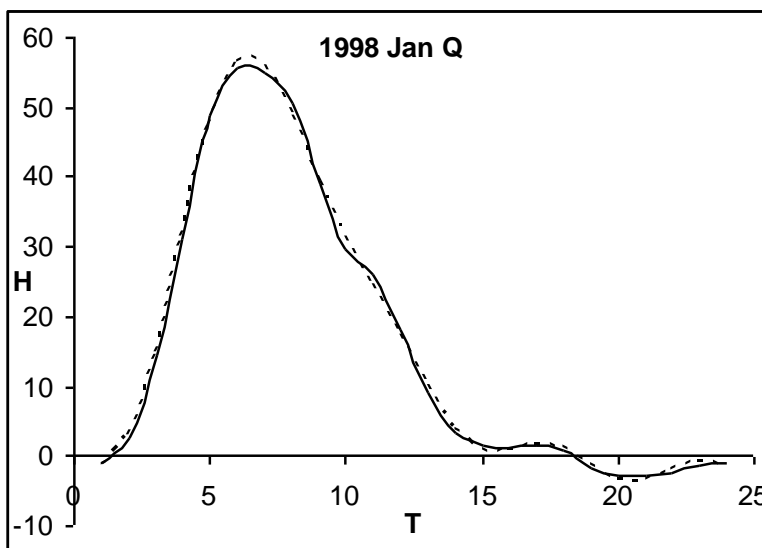


Figure 2: Plot of the measured values of the horizontal component of the earth's magnetic field (indicated by the continuous curve) and the Fourier analysed and reconstructed values (indicated by the dashed curve) for the five magnetically quiet days of January, 1998

Figure 2, is similar to Figure 1, but for January, 1998. As is evident from the figures the agreement between the observed  $\Delta H$  values and the Fourier analysed and reconstructed values are remarkably good.

The observed data values (indicated by “continuous lines”) and the Fourier analysed and reconstructed data values (indicated by “dashed curves”) versus UT is plotted for the month January of the magnetically “disturbed” days for the year 1987 in Figure 3, and for the year 1998 in Figure 4.

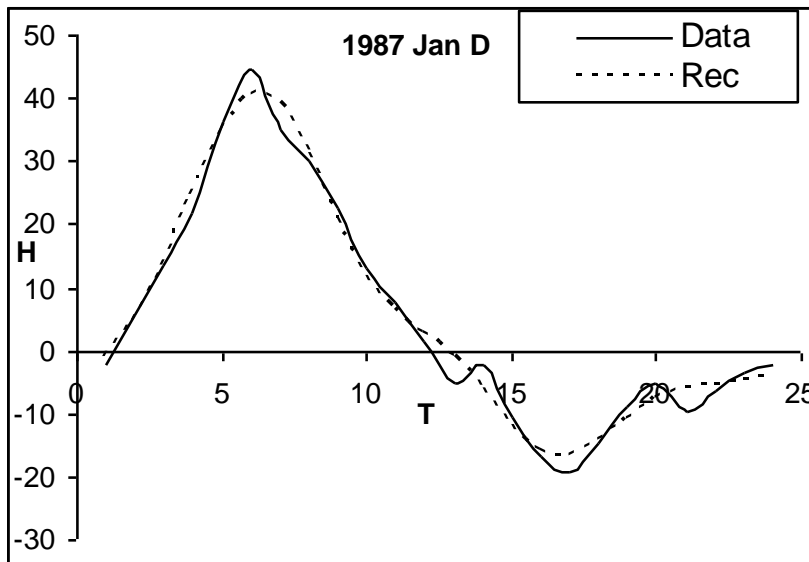


Figure 3: Plot of the measured values of the horizontal component of the earth's magnetic field (indicated by the continuous curve) and the Fourier analysed and reconstructed values (indicated by the dashed curve) for the five disturbed days of January, 1987.

Here too, the H-values reach their maximum between 07 - 08 hours UT as in the case of quiet days. However, in contrast to quiet days, the horizontal component exhibits large excursions on the negative side around local noon before returning to the baseline values. Similar curves were drawn for all the twelve months for the rest of the years.

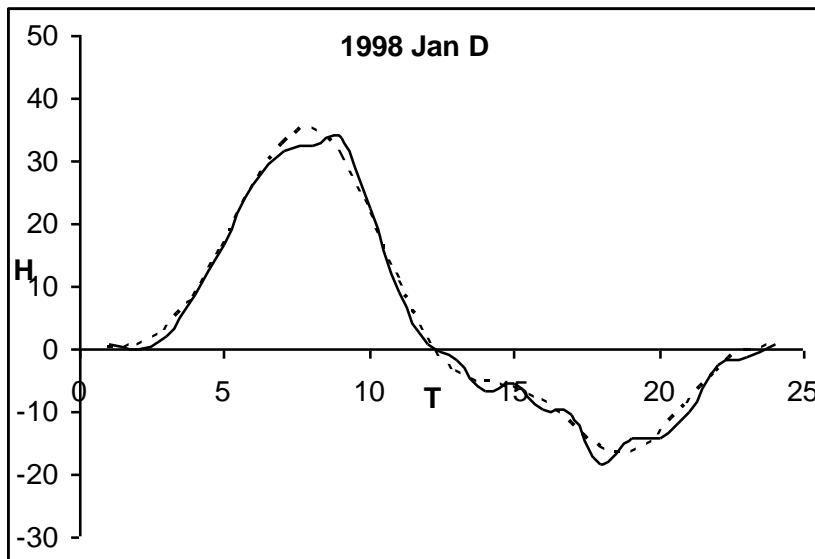


Figure 4: Plot of the observed values of the horizontal component of the earth's magnetic field (indicated by the continuous curve) and the Fourier analysed and reconstructed values (indicated by the dashed curve) for five disturbed days of January, 1998.

### SEASONAL VARIATIONS OF THE COEFFICIENTS

In this section we study the seasonal variations of the coefficients of the Fourier series (3). We follow the Lloyd's seasons [11] and divide the months of the year into three seasons: December or D-season (January, February, November and December), Equinox or E-season (March, April, September and October) and the June solstice or J-season (May, June, July and August).

Thus Figures 5 and 6 are plots of the leading coefficients in the series (5) versus the years studied, with  $A_0$ ,  $A_1$  and  $A_2$  being given in figure 5 and  $B_0$ ,  $B_1$  and  $B_2$  in figure 6. As can be seen from figure 5, the coefficient  $A_0$  which is representative of the background magnetic field is highest during the E- months. The same is true for the second order coefficient  $A_2$ , while the first order coefficient  $A_1$  shows a mixed behavior. On the other hand,  $A_0$  during the D and J months does not show any consistent behavior, with  $A_0$  for the D-months being less than equal to or greater than the  $A_0$  values for the J-months. The same is also true for the coefficients  $A_1$  and  $A_2$  for the D and J-months.

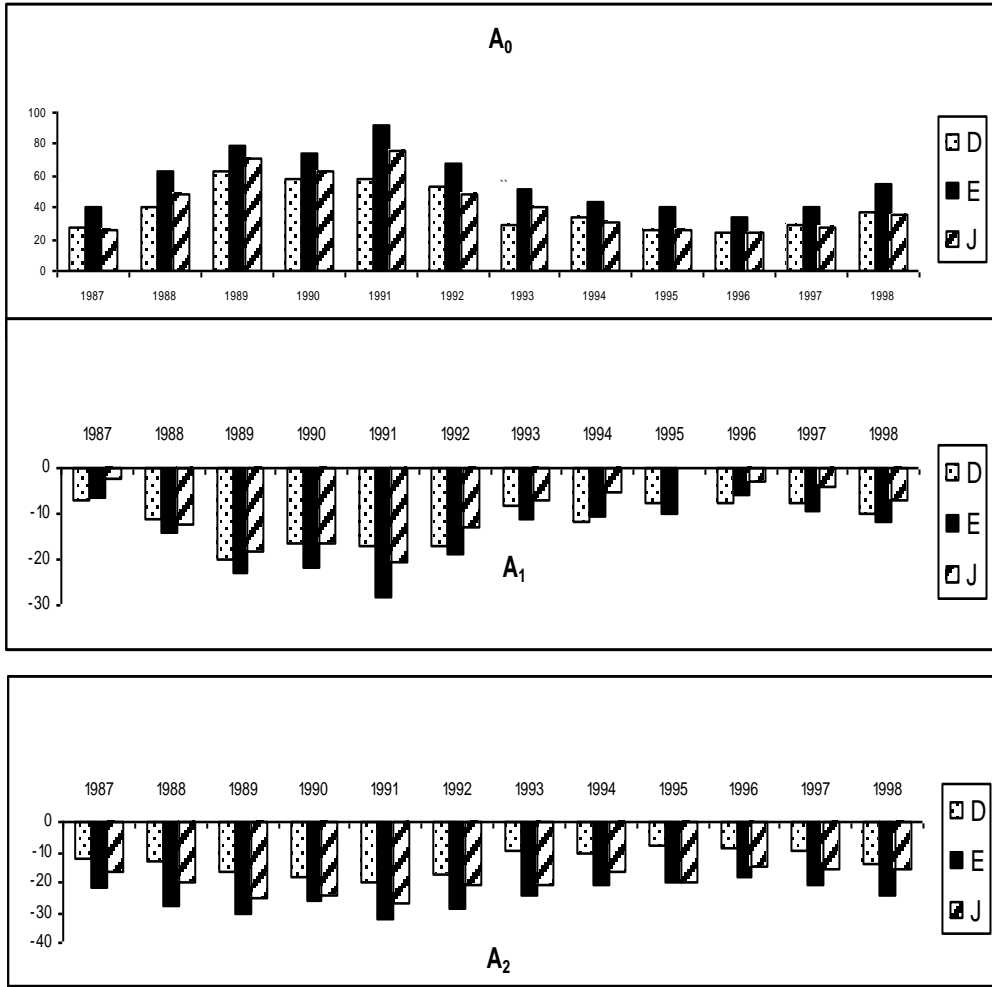


Figure 5: Plot of the variation of the zero ( $A_0$ ), first ( $A_1$ ) and second ( $A_2$ ) order Fourier coefficients of (5) versus time (in years) as a function of the seasons.

Similar to  $A_0$  in figure 5, the coefficient  $B_1$  (figure 6) dominates during the E-months. The same is also true for the third order coefficient  $B_3$ ; while the first order coefficient shows a mixed behavior,  $B_1$  for the J-months is generally greater than  $B_1$  for the D-months (except for 1998 when it is slightly lower). Similarly the coefficients  $B_3$  is generally dominant for the E-months (except for 1995). Also  $B_3$  for the D-months is the least, except for 1992 when it is



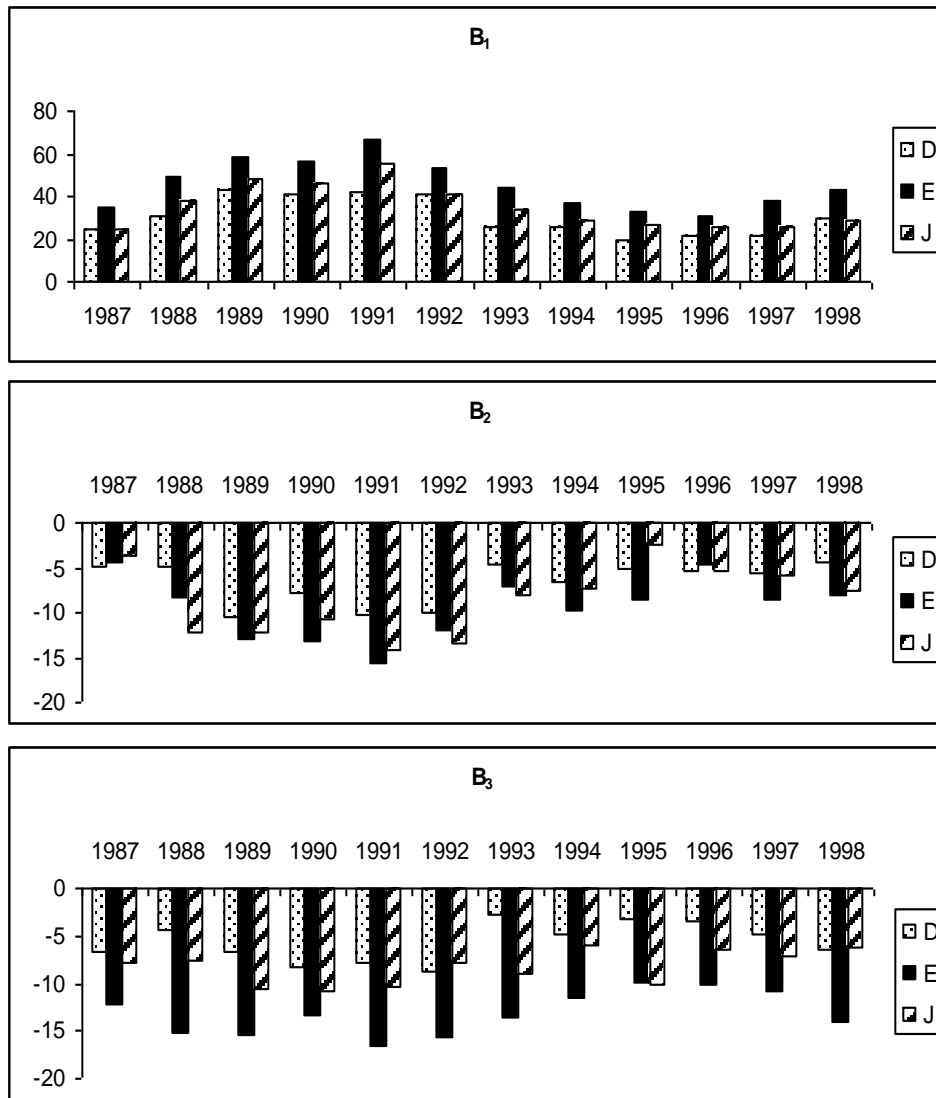


Figure 6: Plot of the variation of the first ( $B_1$ ), second ( $B_2$ ) and third ( $B_3$ ) order Fourier coefficients of (5) versus time (in years) as a function of the seasons.

D-months. Finally, figure 7 depicts the plot of the coefficients  $A_0$  and  $B_1$  with sunspot number for the years 1987-'98. As can be seen from the figure both the coefficients  $A_0$  and  $B_1$  correlate positively with the sunspot number.

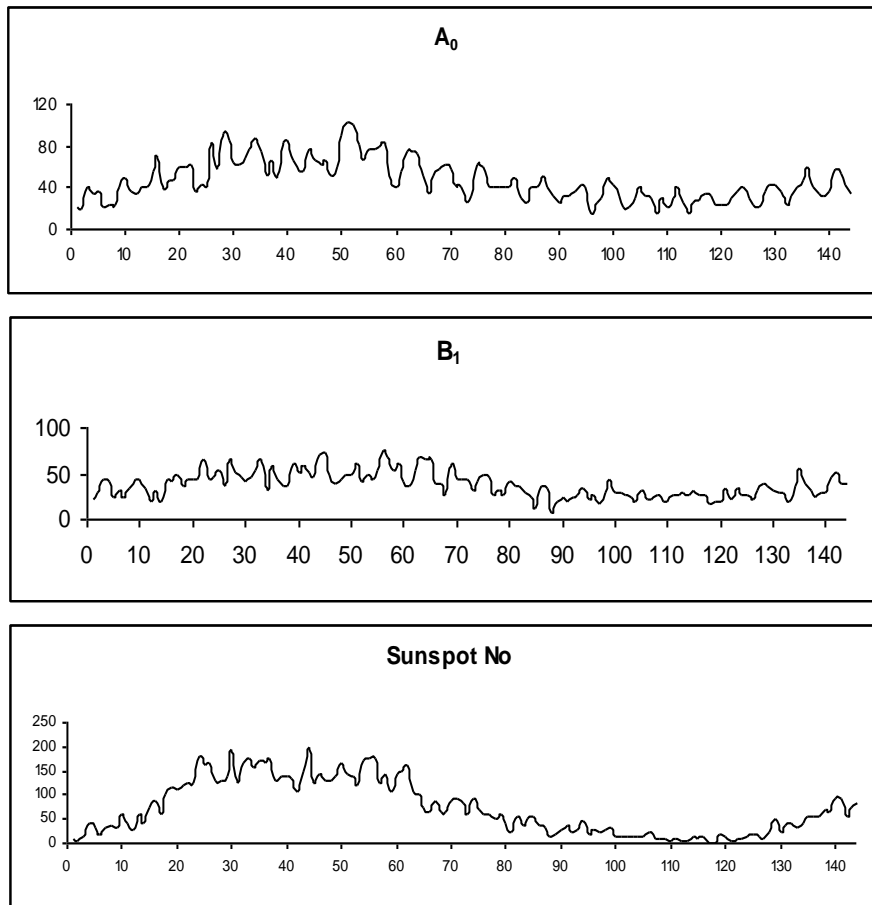


Figure 7: Plot of the Fourier coefficients  $A_0$  and  $B_1$  of (5) and the sun-spot number versus time from 1987 to 1998 (depicted as cumulative months from 0 to 144).

## DISCUSSION

The daily variation of the Earth's magnetic field is known to be generated by solar heating in the upper regions of the atmosphere; this is due to the movement of conductive air across the lines of the magnetic field. However, Schruster [12] and Chapman [13] suggested lunar and solar tides as the cause of air movement in the upper atmosphere, which is associated with the dynamo current and driven by wind and thermal tidal motions in the E-region of the ionosphere. Due to the presence of a non-conducting boundary, a strong vertical polarisation field opposes the downward flow of electric current. This field, in turn, gives rise to an intense Hall current which has been named as the equatorial electrojet (EEJ) [14]. This EEJ flows along the dip equator in the ionospheric E-region on the dayside within a latitudinal belt of  $\pm 3^\circ$  and is responsible for the variations observed in the Earth's magnetic field.

On disturbed days, however, it has been suggested that the enhancement of the field over the magnetic equator during storm sudden commencement is due to the imposition of an additional electric field over the equatorial region, causing additional electrojet currents [15].

An additional mechanism is the thermospheric winds produced by auroral heating during magnetic storms. These westward winds drive an equatorward Pedersen current which ultimately results in the generation of a poleward electric field, a westward  $\bar{E} \times \bar{B}$  drift and an eastward current. This total pattern of disturbance winds, electric fields and currents is superimposed upon the background quiet day pattern [16]. These neutral winds can also spread their influences to lower latitudes even in the absence of electric fields through Joule heating coupled to convective ion drag and Corioli's force [17, 18]. And anomalously high wind speeds have been observed on numerous occasions at mid-latitudes during disturbed conditions.

The zero order coefficients in the Fourier series expansion of the geomagnetic field is a measure of the stationary component present at all times. The plasma densities in the ionosphere vary greatly between day and night as well as with season, solar activity and solar cycle. The daily variation of the electron densities aids the development of ionospheric currents which contribute to the diurnal magnetic field variations observed at the surface; the first order coefficients are thus a measure of this diurnal variation. While it is tempting to interpret the higher periods as artefacts of the Fourier series expansion, it may be noted that thermospheric winds have been observed with periods of 45 and 58 hours; one of the stations' data that contributed to this study was that of Alibag. These thermospheric winds can move ionospheric plasma across geomagnetic field lines creating a dynamo that can set up currents which can modulate the field at these higher periods [19]. As regards variation with season it may be noted that Rastogi and Iyer [20], in a study of the quiet day variations of the geomagnetic field at low latitudes, found the variations in amplitude to be a maximum during the equinoctial months. We also find the Fourier coefficients to be generally larger during the E-months. Finally, in a study of the quiet day geomagnetic field at 21 stations, Yamazaki et. al. [21] have shown that the quiet day variations very emphatically depend on solar activity. While the F10.7 radiation was their proxy for solar activity, we find that the Fourier coefficients (and hence the field deviations) correlate positively with Sun spot number.

## CONCLUSION

We have, in this paper, modelled the horizontal component of the Earth's magnetic field observed at Thiruvananthapuram by Fourier analysis, retaining the first five harmonics in the Fourier expansion. We find that the first five harmonics are sufficient to model the horizontal component of the Earth's magnetic field observed at Thiruvananthapuram, as there is excellent agreement between the observed and the Fourier analysed and reconstructed values on "quiet days"; minor deviations occur on "disturbed days" due to the rapid fluctuations in the H-field on such days.

## ACKNOWLEDGEMENTS

RJ and CVG thank the UGC, New Delhi for a Teacher and Emeritus Fellowship respectively.

## REFERENCES

1. T J Sabaka, N Olsen, and M E Puruckel, 2004 Extending comprehensive models of the Earth's magnetic field with Orsted and CHAMP data . *Geophys. J. Int. doi 1111/j 1365-266X.2004.02421.x*
2. W H Campbell and E R Schiffmacher 1985. Quiet ionospheric currents of the northern hemisphere derived from geomagnetic field records. *J. Geophys Res.*, 90, 6745 - 6486.
3. W H Campbell and E R Schiffmacher 1988 Quiet ionospheric currents of the southern hemisphere derived from geomagnetic field records. *J. Geophys Res.*, 93, 933 - 944.
4. L Alldredge 1981. Rectangular harmonic analysis applied to the geomagnetic field. *J. Geophys. Res.*, 86, 3021 - 3026.
5. G V Haines 1985. Spherical cap harmonic analysis. *J. Geophys. Res.*, 90, 2583 – 2591
6. M Korte and R Holme 2003 Regularization of spherical cap harmonics. *Geophys. R. Int.* 153, 253 – 262.
7. E Thebault, J Schott. M Manda and J Hoffbeck 2005. A new proposal for spherical cap harmonic modeling. *Geophys. J. Int.* 159 83 – 103.
8. M Holschneider, A Chambodut and M Manda 2003. From global to regional analysis of the magnetic field on the sphere using wavelet frames. *Phys. Earth Planets In.* 135 107 – 124.

9. P R Sutcliff 1999 The development of a regional geomagnetic daily variation model using neural networks. *Ann. Geophysicae*, 18, 120 - 128.
10. A B Rabiou, A I Mamukuyomi and E O Joshua, 2007. Variability of equatorial ionosphere inferred from geomagnetic field measurements. *Bull. Astr. Soc. India*, 35, 607 - 618.
11. F Eleman, 1973. *Cosmical Geophysics, ed. Egeland A et al, Scandinavian University Books, Oslo, Chapter 3, 45.*
12. A Schruster, 1908 The diurnal variation of terrestrial magnetism. *Philos. Trans. Roy. Soc. London A*. 208 163 – 204.
13. S Chapman, 1919 The solar and lunar diurnal variations of terrestrial magnetism. *Philos. Trans. Roy. Soc. London A*. 218, 1 – 118.
14. S Chapman, 1951 The equatorial electrojet as detected from the abnormal electric current distribution above Huancayo and elsewhere. *Arch. Meteorol. Geophys. Bioclimatol. A* 4, 368 – 392.
15. S Rastogi, 1976. Equatorial E-region electric field changes associated with a geomagnetic storm sudden commencement. *J. Geophys. Res.* 81 687 – 689
16. M Blanc, and A D Richmond, 1980. The ionospheric disturbance dynamo. *J. Geophys. Res.* 85, 1669 – 1686.
17. P W Roper, and A J Baxter, 1978 The effect of auroral energy input and ion drifts in the thermosphere. *J. Atmos. Terr. Phys.* 40 585 - 599
18. M Strauss, 1978 Dynamics of the thermosphere at high latitudes. *Rev. of Geophys.* 16 183 – 194.
19. M Takeda and Y Yamada, 1989 Quasi Two-Day Period Variation of the Geomagnetic Field. *J Geomag. Geoelectr.* 41 469 – 478
20. R G Rastogi and K N Iyer, 1976 Quiet day variation of the geomagnetic H-field at low latitudes. *J. Geomagnetn. Geoelectr.* 28, 461 - 479.
21. Y Yamazaki, et. al., 2011. An empirical model of the quiet daily geomagnetic field variation. *J. Geophys. Res.* v. 116 doi: 10.1029 / 2011 JA 016487